Hydrol. Earth Syst. Sci., 27, 673–687, 2023
https://doi.org/10.5194/hess-27-673-2023

Hydrology and Earth System Sciences
Open Access
EGU

Spatial variability in Alpine reservoir regulation: deriving reservoir operations from streamflow using generalized additive models

Manuela Irene Brunner[1,2,3,4] **and Philippe Naveau**[5]

[1]WSL Institute for Snow and Avalanche Research SLF, Davos, Switzerland
[2]Institute for Atmospheric and Climate Science, ETH Zurich, Zurich, Switzerland
[3]Climate Change, Extremes and Natural Hazards in Alpine Regions Research Center CERC, Davos, Switzerland
[4]Institute of Earth and Environmental Sciences, University of Freiburg, Freiburg, Germany
[5]Laboratoire des Sciences du Climat et l'Environnement (LSCE, EstimR) CNRS, Gif-sur-Yvette, France

Correspondence: Manuela Irene Brunner (manuela.brunner@env.ethz.ch)

Received: 27 June 2022 – Discussion started: 18 July 2022
Revised: 3 January 2023 – Accepted: 21 January 2023 – Published: 2 February 2023

Abstract. Reservoir regulation affects various streamflow characteristics, from low to high flows, with important implications for downstream water users. However, information on past reservoir operations is rarely publicly available, and it is hardly known how reservoir operation signals, i.e. information on when water is stored in and released from reservoirs, vary over a certain region. Here, we propose a statistical model to reconstruct reservoir operation signals in catchments without information on reservoir operation. The model uses streamflow time series observed downstream of a reservoir that encompass a period before and a period after a known year of reservoir construction. In a first step, a generalized additive model (GAM) regresses the streamflow time series from the unregulated pre-reservoir period on four covariates including temperature, precipitation, day of the year, and glacier mass balance changes. In a second step, this GAM, which represents natural conditions, is applied to predict natural streamflow, i.e. streamflow that would be expected in the absence of the reservoir, for the regulated period. The difference between the observed regulated streamflow signal and the predicted natural baseline should correspond to the reservoir operation signal. We apply this approach to reconstruct the seasonality of reservoir regulation, i.e. information on when water is stored in and released from a reservoir, from a dataset of 74 catchments in the central Alps with a known reservoir construction date (i.e. date when the reservoir went into operation). We group these reconstructed regulation seasonalities using functional clustering to identify groups of catchments with similar reservoir operation strategies. We show how reservoir management varies by catchment elevation and that seasonal redistribution from summer to winter is strongest in high-elevation catchments. These elevational differences suggests a clear relationship between reservoir operation and climate and catchment characteristics, which has practical implications. First, these elevational differences in reservoir regulation can and should be considered in hydrological model calibration. Furthermore, the reconstructed reservoir operation signals can be used to study the joint impact of climate change and reservoir operation on different streamflow signatures, including extreme events.

1 Introduction

Reservoir regulation affects various streamflow characteristics – including variability (Eisele et al., 2004; Ferrazzi et al., 2019), seasonality (Biemans et al., 2011; Adam et al., 2007; Rottler et al., 2019), and extreme events (Verbunt et al., 2005; He et al., 2017; Wang et al., 2017; Wan et al., 2017; Vicente-Serrano et al., 2017; Mahe et al., 2013; Tijdeman et al., 2018; van Oel et al., 2018; Volpi et al., 2018; Brunner, 2021) – in almost 50 % of the world's large rivers ($> 1000\,\mathrm{m^3\,s^{-1}}$) and in 8 % of the rivers overall (Lehner et al., 2011). Regulation pat-

terns may vary across regions and hydro-climates, as reservoirs are operated for different purposes including irrigation, energy production, water supply, and recreation and, in some cases, in a multi-purpose way (Lehner et al., 2011; Brunner et al., 2019a). However, information on these reservoir operation signals, i.e. on when water is stored in and when it is released from reservoirs, is hardly publicly available, despite its importance for model calibration and impact assessments (Yassin et al., 2019; Speckhann et al., 2021; Brunner et al., 2021; Steyaert et al., 2022). In some cases, reservoir operation records are made available by the operating agencies (e.g. Steyaert et al., 2022); however, this is the exception rather than the rule. As a consequence, it is often unclear how reservoir regulations vary across a region and whether and how the regulation patterns are related to catchment characteristics – knowledge that might be useful to transfer reservoir regulation information to basins without such information. Because of the lack of reservoir regulation information, hydrological and land surface models often use generic reservoir operation schemes that do not necessarily reflect local behaviour, which is particularly problematic when simulating streamflow at sub-monthly resolution or when modelling extreme events (Hanasaki et al., 2006; Yassin et al., 2019; Turner et al., 2021).

Various attempts have been made to infer reservoir operation signals from different types of data sources, including optical and altimetry remote sensing (Peng et al., 2006; Eldardiry and Hossain, 2019; Hou et al., 2022; Du et al., 2022), reservoir purpose, simulated inflows and water withdrawals (Hanasaki et al., 2006; Voisin et al., 2013), or in- and outflows (Turner et al., 2021). To identify the timescales most affected by reservoir operation, White et al. (2005) and Shiau and Huang (2014) used the wavelet transform on both observed in- and outflow time series and compared their wavelet power spectra. To estimate reservoir release policies, Coerver et al. (2018) used fuzzy rules to link inflow and storage with reservoir release for a set of reservoirs in Asia and North America, and Turner et al. (2021) developed harmonic regression models using observed and simulated daily reservoir in- and outflows for large reservoirs in the continental United States (Steyaert et al., 2022). To map input–output relationships for dams around the world, Ehsani et al. (2016) used artificial neural networks and data on inflow, release, and storage. While these approaches are very helpful for reservoir signal reconstruction in case both in- and outflow data are available, inferring the reservoir operation signal based on outflow information only remains challenging.

Here, we propose a statistical three-step approach for reservoir signal reconstruction in catchments where reservoir outflow time series are available. The approach is based on a generalized additive model (GAM) that enables reconstructing reservoir operation signals from observed streamflow time series measured downstream of a reservoir or a set of reservoirs and encompasses the period before and after a known year of reservoir construction. In a first step, the approach fits a GAM to streamflow observations representing natural pre-reservoir conditions using precipitation, temperature, day of the year, and glacier mass balance changes as covariates. In a second step, this GAM is applied to covariates derived for the regulated post-dam period to predict natural streamflow for this regulated period. In a last step, the reservoir regulation signal is reconstructed by subtracting the predicted "natural signal" from the observed regulated signal. This resulting signal indicates how much water is stored in and released from reservoirs in which season (i.e. day of the year). These reservoir–storage–seasonality signals take a reservoir perspective and provide information on storage in addition to releases but not on inflow. Therefore, they are distinct from the signals extracted through other approaches, e.g. simulated water releases (Coerver et al., 2018), spectral differences between in- and outflows highlighting the timescales most affected by reservoir regulation (White et al., 2005; Shiau and Huang, 2014), or water storage and release policies, which define release decisions as percent deviations from long-term mean inflow (Turner et al., 2021). Our approach can be used to reconstruct reservoir operation signals in catchments where streamflow and climate data are available for a period before and after a known date of reservoir construction. Such information is more widely available than reservoir in- and outflow measurements, which means that the approach is applicable in different regions around the globe where streamflow observations and information on reservoir construction dates are available.

Here, we use the proposed approach to shed light on spatial variations in reservoir regulation signals and their relationship to catchment characteristics. To do so, we apply the approach to extract reservoir signals from observed time series of 74 catchments in the central Alps (Sect. 2.2). From this database of 74 extracted signals, we identify groups of catchments with similar reservoir operation strategies using functional data clustering (Sect. 2.3; Chebana et al., 2012; Ternynck et al., 2016). The functional form is derived from discrete observations (Ramsay and Silverman, 2002), either by smoothing the data non-parametrically (Jacques and Preda, 2014) or by projecting the data onto a set of basis functions. The basis function (e.g. B spline, Fourier, or wavelet bases) coefficients can be used for clustering (Cuevas, 2014). It has been shown in previous studies that functional data representations can be beneficial for identifying groups of similar hydrographs over a range of temporal scales, such as spring flood events (duration of 6 months; Ternynck et al., 2016), flood events (duration of several days; Brunner et al., 2018), low-flow events (Laaha et al., 2017), diurnal discharges (duration of 1 d; Hannah et al., 2000), yearly hydrographs (Merleau et al., 2007; Jamaludin, 2016), and streamflow regimes (Brunner et al., 2020). Here, we use functional data clustering to identify groups of catchments with similar reservoir operation seasonalities. We then assess whether and how catchments with different reservoir operation strategies differ in their location and catchment charac-

teristics. The combination of the proposed reservoir signal reconstruction approach with functional clustering allows us to provide insights into how reservoir regulation varies spatially in the Alps and to which degree these variations are related to catchment characteristics.

2 Methods

2.1 Dataset

The central Alps are an interesting region for studying different reservoir regulation patterns because this region is characterized by diverse hydro-climatic regimes (Bard et al., 2015) which are often heavily influenced by reservoirs (Lehner et al., 2005; Brunner et al., 2019a). Therefore, we identify a large sample of 74 regulated catchments in the headwater regions of the four major European rivers originating in the central Alps, namely the Rhine, Rhône, Danube, and Po, for which the date of reservoir construction, i.e. the date when a reservoir went into operation, is known and for which observed daily streamflow data are available for both a period before and a period after reservoir construction (Fig. 1). The observed streamflow time series were obtained from national agencies in Switzerland (Federal Office for the Environment, FOEN), Austria (Austrian Ministry of Sustainability and Tourism), and eastern France (Banque HYDRO) and regional agencies in southern Germany (regions of Bavaria, Bavarian State Office for the Environment, and Baden-Württemberg, State Institute for the Environment Baden-Württemberg). The streamflow records of the different catchments do not necessarily cover the same time period; however, each catchment has streamflow data for at least 10 years before and after reservoir construction (see Fig. 2, for an example time series in the Swiss Alps). Northern Italy was excluded from the analysis because streamflow records provided by the regional agencies did not cover the pre-reservoir construction period.

In addition to streamflow, we derive daily meteorological time series (precipitation and temperature) for each catchment from the gridded observational E-OBS dataset at 25 km spatial resolution for the period 1950–2020 (Cornes et al., 2018) by averaging over all grid cells within a catchment. If present, missing values in the time series of all variables are replaced by the daily mean over the natural period for the natural data and over the regulated period for the regulated data. Temperature and precipitation time series are smoothed over a moving time window of 5 d to remove noise because smoothing improves model performance. Furthermore, data on reservoir locations and construction dates are also obtained from national agencies (FOEN in Switzerland, the Austrian Ministry of Sustainability and Tourism in Austria, and the Comité Fran¿ais des Barrages et Réservoirs in France; https://www.barrages-cfbr.eu/, last access: 1 March 2022) and open-source databases (for Germany; see

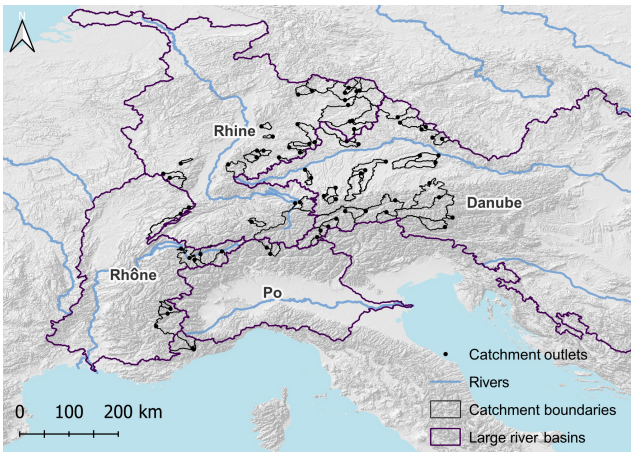

Figure 1. A total of 74 catchments in the central Alps with at least 10 years of streamflow data before and after reservoir construction (black catchment outlines).

Speckhann et al., 2021). To account for changes in glacier melt contributions over time, we compute annual glacier mass balance changes for each of the selected catchments using simulated mass balance changes over the period 1951–2020 for the glaciers in the Randolph Glacier Inventory (RGI Consortium, 2017; Compagno et al., 2021). After estimating the average mass balance change for each glacier in a catchment by weighting changes across different elevation bands, each annual mass balance time series is disaggregated into daily resolution by smoothing the annual signals over 365 d. This smoothing avoids step-like features in the mass balance change time series.

2.2 Reservoir signal reconstruction using GAMs

Here, we propose a modelling approach to reconstruct the reservoir operation signal from observed streamflow time series measured downstream of a reservoir before and after reservoir construction, representing natural and regulated conditions, respectively (Fig. 3a and b). Before the reservoir construction date, a regression scheme can learn the natural link between streamflow times series and some appropriate meteorological explanatory variables. In this work, this natural baseline signal is obtained by applying a generalized additive model (GAM; Hastie and Tibshirani, 1986) during the pre-reservoir time period. After the reservoir construction, the reservoir operation signal can be defined as the difference between the regulated streamflow time series and the signal that would have been measured without the reservoir. The latter signal was never observed, but it can be estimated by applying the learning GAM link to post-reservoir meteorological explanatory variables.

Generalized additive models (GAMs) extend the linear regression set-up and therefore represent a flexible model structure to predict streamflow. The classical additive linear

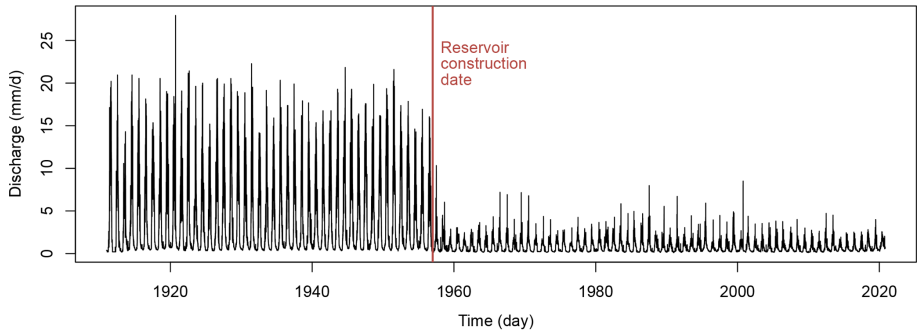

Figure 2. Streamflow time series for the catchment of the Dranse de Bagnes (gauge Le Châble) illustrating streamflow changes induced by the construction of the Mauvoisin reservoir in 1957.

link, $\sum \beta_j X_j$, between the observational vector $\boldsymbol{Y}$ and the explanatory variables $(X_1, \ldots, X_p)^T$ is replaced by a sum of smooth functions $\sum f_j(X_j)$ (see, for example, Hastie and Tibshirani, 1986). Hence, GAMs represent nonlinear relationships between covariates and the target variable. Each smooth function $f_j(.)$ corresponds to a linear projection on a given basis, which is here a cubic smoothing spline representation (see, for example, Hastie and Tibshirani, 1986; Wood, 2017). Typically, a GAM is written as follows:

$$y_t = \sum_{j=1}^{p} f_j\left(x_{tj}\right) + \sigma \epsilon_t, \tag{1}$$

where $\sigma > 0$, and ϵ_t represents a standardized random noise. In this study, the response variable y_t corresponds to streamflow time series in millimetres per day ($\mathrm{mm\,d^{-1}}$). Alternatively, GAMs have, in the context of reservoirs, also been used to predict variables other than streamflow such as eutrophication levels (Catherine et al., 2010) or downstream water temperatures (Coleman et al., 2021). The index t represents the time evolution in days and spans the time period before reservoir construction, which varies by catchment. For example, the construction of the Mauvoisin reservoir in 1957 can be clearly identified in the streamflow time series of the catchment Dranse de Bagnes (gauge Le Châble; Fig. 2). In this study, the set of explanatory variables, $(X_1, \ldots, X_p)^T$, contains three climatological parameters including temperature, precipitation, seasonality (day of year), and modelled glacier mass balance changes. During the unregulated pre-reservoir period, the GAM learns the nonlinear relationship between streamflow time series and corresponding climatological parameters. Then, the estimated transfer function f_j calibrated on the unregulated period is applied via Eq. (1) to the regulated period to predict natural streamflow. The approach relies on the assumption that the relationship between climate variables and streamflow remains stable over time. The main advantage of GAMs is that cubic spline modelling offers flexibility for each covariate and goes beyond a restrictive linear regression framework, while the additive structure among covariates remains simple. This balance between non-parametric modelling and a simple additive link facilitates the interpretation of the contribution of each explanatory variable. Still, other regression techniques (neural networks, random forest, and other machine learning algorithms) could replace our GAM approach in the scheme displayed in Fig. 3. Keeping in mind that our training period can be short (a few decades) at some locations, this lack of a large training dataset may also limit the application of fully data-driven machine learning techniques.

The model covariates include the following three climatological drivers: (1) smoothed daily temperatures, (2) smoothed daily precipitation, and (3) day of the year (seasonality) and interpolated daily glacier mass balance changes (Fig. 3a; for details on datasets, see Sect. 2.1). The last variable takes into account non-stationarities induced by changing glacier melt. Discharges during the natural and regulated period can have different magnitudes as a result of water diversions, e.g. in the case of hydropower production. Therefore, we normalize both the natural and regulated streamflow time series by dividing by the mean flow over the corresponding period. Such normalization makes natural and regulated flow magnitudes comparable. All other variables were used on their original scales. We use these covariates to fit a GAM for the prediction of streamflow under natural flow conditions (Fig. 3b). To do so, we fit the GAM to the streamflow observations of the pre-dam period. As positive and skewed random variables, it is unlikely that streamflow time series follow a Gaussian distribution given the four covariates. To handle this issue, we choose a gamma family within the GAM approach and study the following additive link:

$$f_1\left(p_t\right) + f_2\left(h_t\right) + f_3\left(d_t\right) + f_4\left(g_t\right), \tag{2}$$

where p_t corresponds to smoothed precipitation, h_t to smoothed temperature, d_t to the day of the year, and g_t to the interpolated glacier mass balance changes (for the implementation, we used the R package mgcv; Wood, 2022, 2017). We assess the model's performance by comparing observed with predicted streamflow values and by computing a range of different performance metrics including the Kling–Gupta (KGE) and Nash–Sutcliffe efficiencies (NSE)

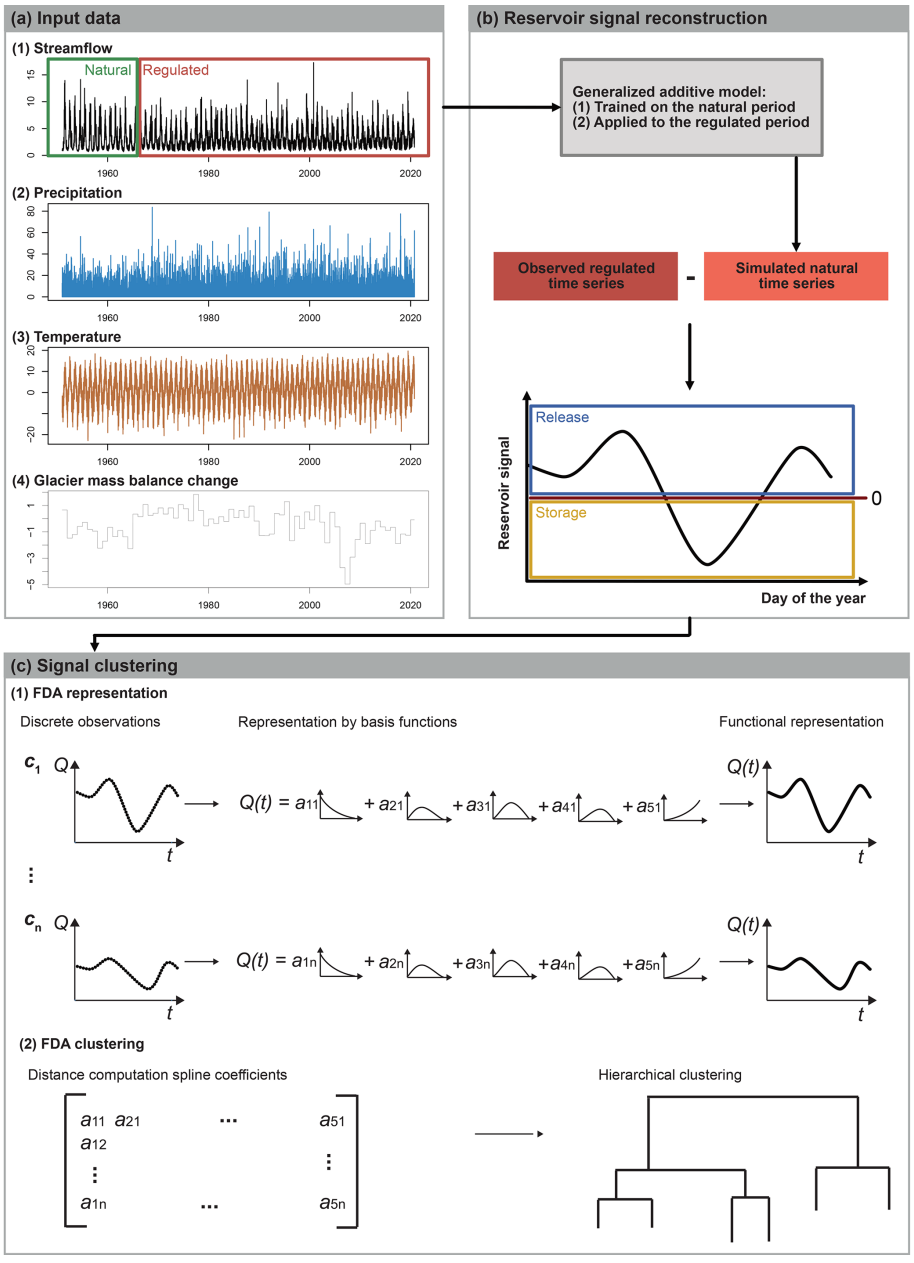

Figure 3. Workflow illustration. **(a)** Input data used to fit and run the generalized additive model (GAM), including streamflow, precipitation, temperature, and glacier mass balance changes for a period before and after reservoir construction representing natural and regulated conditions, respectively. **(b)** GAM fitting using the natural data before reservoir construction. GAM is used to predict the natural signal for the regulated period, and the regulation signal is reconstructed by subtracting the predicted "natural time series" from the observed regulated time series (i.e. determining the seasons with reservoir storage and release). **(c)** Reservoir signal clustering using functional data analysis (FDA), using hierarchical clustering on functional representations (i.e. spline basis functions) of the reconstructed signals of all catchments in the dataset.

(Gupta et al., 2009; Nash and Sutcliffe, 1970), volumetric efficiency (VE, Criss and Winston, 2008), mean absolute error (MAE), root mean squared error (RMSE), and percent bias (PB). The model captures the observed values and their distribution quite well, as illustrated by comparisons of observed vs. predicted values, observed and predicted quantiles, and observed and predicted time series (for an example catchment, see Fig. 4). This visual impression is confirmed by the goodness-of-fit statistics computed across all 74 catchments (Table 1). KGE values range between a first quartile of 0.38 and a third quartile of 0.75, NSE values between 0.23 and 0.64, and volumetric efficiencies between 0.49 and 0.73,

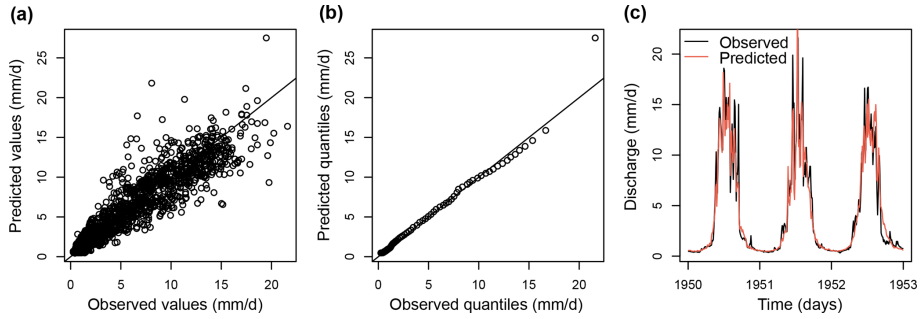

Figure 4. Evaluation of the GAM model fitted using natural streamflow data of the Dranse de Bagnes (before reservoir construction 1911–1956) and used to predict streamflow with precipitation, temperature, day of year, and glacier mass balance changes as predictors. **(a)** Observed vs. predicted values (1911–1956), **(b)** Q–Q plot of observed vs. simulated quantiles (1911–1956), and **(c)** observed vs. predicted time series (3 years; 1950–1953).

Table 1. Performance of GAM in predicting natural streamflow for the pre-regulation period across catchments quantified by different goodness-of-fit statistics including the Nash–Sutcliffe efficiency (NSE; values between 0–1 with an optimum at 1), Kling–Gupta efficiency (KGE; values between 0–1 with an optimum at 1), volumetric efficiency (VE; values between 0–1 with an optimum at 1), mean absolute error (MAE; $\mathrm{mm\,d^{-1}}$), root mean squared error (RMSE; $\mathrm{mm\,d^{-1}}$), and percentage bias (PB; %).

Statistic	First quartile	Median	Mean	Third quartile
KGE	0.38	0.48	0.53	0.75
NSE	0.23	0.31	0.34	0.64
VE	0.49	0.56	0.58	0.73
MAE	0.27	0.44	0.42	0.51
RMSE	0.45	0.77	0.84	0.96
PB	0	0	0	0

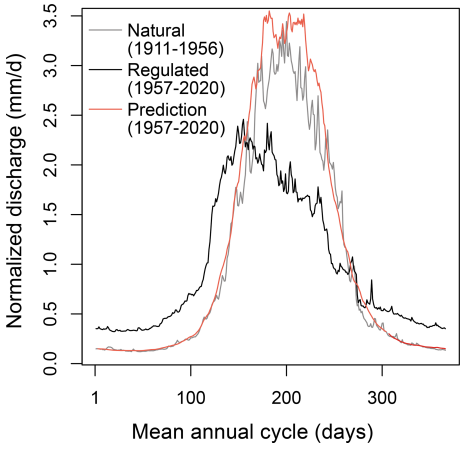

Figure 5. Comparison of the observed natural streamflow regime (i.e. the mean annual hydrograph) of the Dranse de Bagnes before reservoir construction (grey; 1911–1956), observed regulated regime after reservoir construction (black; 1957–2020), and simulated natural regime for the period after reservoir construction (red; 1957–2020).

which means that mean flows and volumes are slightly better simulated than high flows. MAEs range between 0.27 and 0.51 $\mathrm{mm\,d^{-1}}$ (normalized flow), the RMSEs between 0.45 and 0.96, and the percentage bias is 0. This performance assessment suggests that the model is suitable for predicting streamflow under natural conditions. Model performance is independent of the length of the record available to fit the GAM but depends on catchment area and elevation (Fig. B1). The best performance is achieved in large and high-elevation catchments, while performance is worst in small and low-elevation catchments.

Next, we apply this model to deduce the never-observed "natural" flow after the reservoir construction. In this case, the GAM inputs are the same four covariables, i.e. temperature, precipitation, day of year, and glacier mass balance changes, but taken over the period after the reservoir construction. As an application example, Fig. 8 compares the natural streamflow regime (i.e. the mean annual hydrograph) of the Dranse de Bagnes derived using the model for the regulated period (red) with the natural observed (grey) and the regulated observed streamflow regimes (black). The observed regulated regime has a seasonality distinct from the simulated natural regime. We assume that the difference between the observed regulated streamflow signal and the predicted natural baseline represents the reservoir operation signal.

Under this assumption, we derive the reservoir operation signal by subtracting the predicted natural signal from the observed regulated signal (Fig. 6a). To remove noise and retrieve a clear signal, we smooth the signal using regression splines (Fig. 6b). Positive values represent release conditions, as the observed regulated signal is higher than the predicted natural signal, while negative values represent storage conditions, as the predicted natural signal would be higher than the actually observed regulated signal. The reconstructed signal informs about regulation at a daily scale but can also be

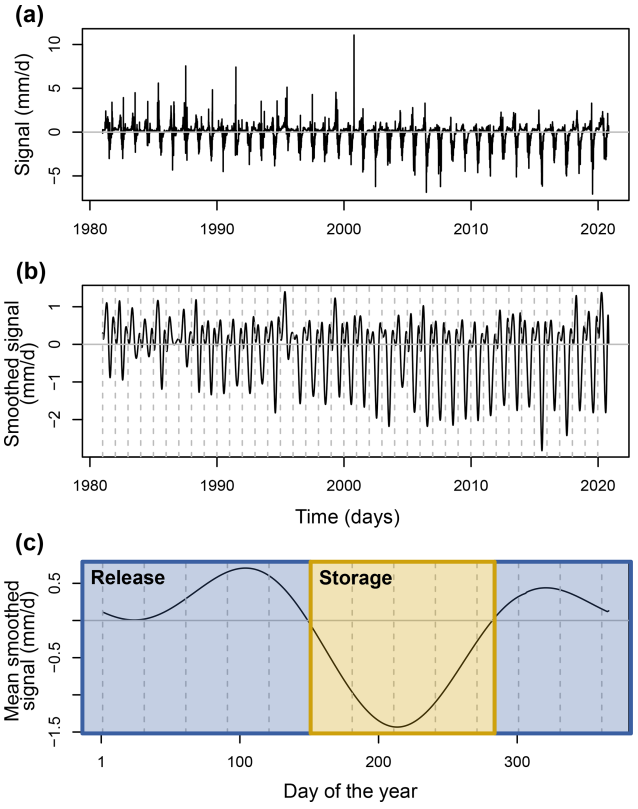

Figure 6. Reservoir signal for the Dranse de Bagnes reconstructed for the period 1960–2020 using the GAM predictions by subtracting predicted natural discharge from observed regulated discharge, where positive and negative values indicate release and storage, respectively. **(a)** Raw daily signal. **(b)** Smoothed signal (spline smoothing). **(c)** Mean seasonal signal.

aggregated to mean daily values to represent regulation seasonality, i.e. the regulation regime. We here derive reservoir regulation seasonality by averaging the reconstructed daily signals for each day of the year (Fig. 6c).

A direct evaluation of the extracted seasonal reservoir signals is unfortunately not possible because observed inflow and outflow data are not publicly available. Therefore, we evaluated the approach using an alternative validation strategy. The Swiss Federal Office of Energy provides weekly reservoir storage estimates aggregated over a larger region (i.e. canton; Bundesamt für Energie BFE, 2022). We use these regional storage estimates to compute seasonal changes in regional storage. We then use the regional storage change curves derived for the regions Valais, Grisons, and Ticino to evaluate the reservoir signals extracted using the GAM for all catchments located in the three regions (Fig. 7). That is, we apply the GAM approach to the catchments located in the cantons Valais, Grisons, and Ticino using temperature, precipitation, and glacier mass balance changes as covariables. We then compare the extracted reservoir regulation signals to the reservoir signals extracted from the regional storage curves. The regulation signal estimates for the 10 catchments using the GAM approach compare very well to the signals derived from observed regional reservoir storage data.

2.3 Reservoir signal variation analysis

We apply the GAM modelling approach introduced in the section above to reconstruct the mean reservoir signals (i.e. reservoir seasonality) of 74 catchments in the central Alps with streamflow data for a period before and after reservoir construction. We then use these reconstructed reservoir seasonalities to identify groups of catchments with similar reservoir operation patterns using functional data clustering (Ramsay and Silverman, 2002) (Fig. 3c). To do so, we follow the approach proposed by Brunner et al. (2020) to cluster streamflow regimes, i.e. mean annual streamflow hydrographs. First, we project the discrete observations, i.e. the reconstructed reservoir operation seasonalities at daily resolution, to a set of B-spline basis functions (R-package fda; Ramsay et al., 2014). B-spline functions are defined by their order of polynomial segments and the number of knots, which determine their ability to represent sharp features in a curve (Höllig and Hörner, 2013). Similar to Brunner et al. (2020), we use five spline basis functions of order four, which corresponds to a minimal number of basis functions still allowing for sufficient flexibility in representing diverse shapes of reservoir operation seasonalities. The projection of the observed reservoir operation seasonalities to the five basis functions results in five coefficients per observed operation signal, with one per spline base. The analysis is performed in R using the packages fda.usc (Febrero-Bande and Oviedo de la Fuente, 2012) and fda (Ramsay et al., 2014). Second, we compute a Euclidean distance matrix using the matrix of $n = 74 \times 5$ spline coefficients. Third, we use a hierarchical clustering algorithm (hclust) with Ward's minimum variance criterion, which minimizes the total within-cluster variance (Ward, 1963). We cut the tree at $k = 2$ clusters because this seems to be the most suitable number of clusters, given the symmetry of the tree. After cluster identification, we assess various properties of the catchments in the different clusters including the natural streamflow regime, catchment area, and catchment elevation.

3 Results of the reservoir signal variation analysis

Reservoir operation in the central Alps varies by season and across catchments, and the types of reservoir signals extracted using the GAM approach can be grouped into two classes (Figs. 8a, b and 9a). In catchments belonging to cluster 1, seasonal flow redistribution from summer to winter is much more pronounced than in catchments belonging to cluster 2. This seasonal redistribution pattern seems to be related to the natural flow regime, which has a more pronounced seasonality in catchments belonging to clus-

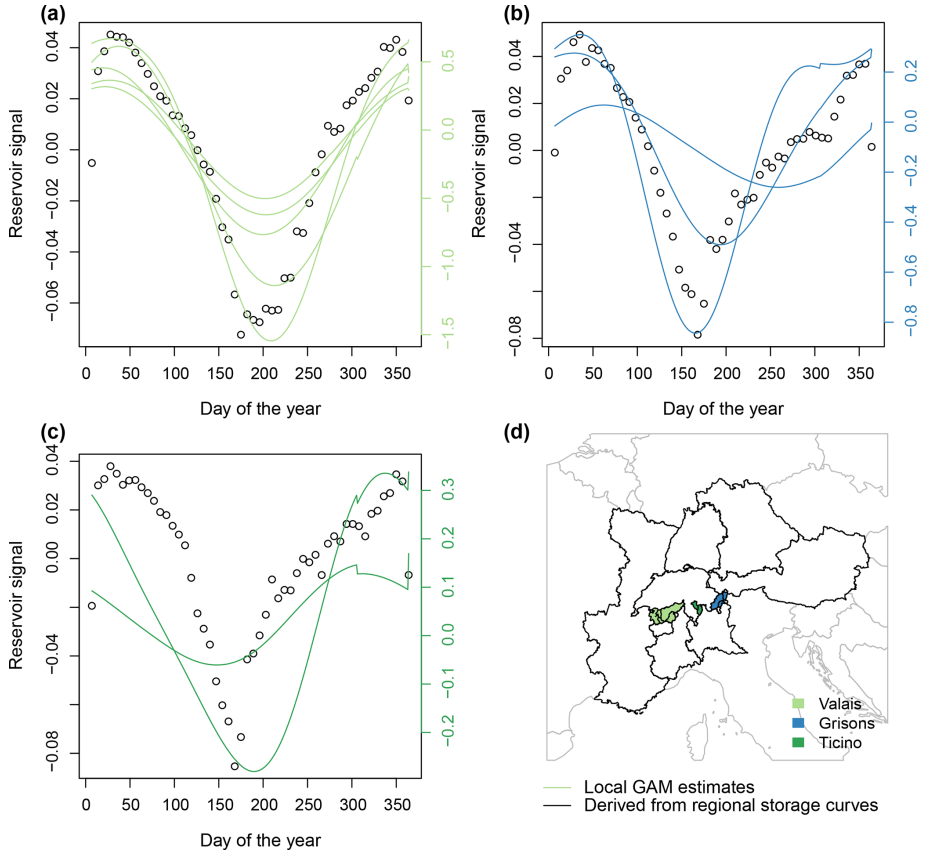

Figure 7. Regional reservoir storage change curves for the regions **(a)** Valais, **(b)** Grisons, and **(c)** Ticino derived from regional reservoir storage data provided by the Swiss Federal Office of Energy compared to the reservoir regulation signals estimated using the GAM of the catchments located in the corresponding cantons **(d)**. **(a)** Rhône, Porte-du-Scex, Rhône, Sion, Rhône, Branson, Dranse de Bagnes, Le Châble, and Vispa, Visp. **(b)** Inn, Tarasp, Inn, Martina, and Spöl, Punt dal Gall. **(c)** Brenno, Loderio and Moesa, Lumino.

ter 1 than those belonging to cluster 2 (Fig. 8c and d). The catchments with stronger seasonal redistribution are located at higher elevations and have larger storage capacities than catchments with weaker seasonal redistribution (Fig. 9c and d) but do not differ in terms of catchment area (Fig. 9a). While some catchments are strongly regulated (i.e. those with strong signal amplitudes), less water is stored and released in other catchments (i.e. those with weak amplitudes; Fig. 8a and b). Independent of magnitude, the seasonal release–storage signal appears to be similar in most catchments. Water is mostly stored in summer (negative values), when snowmelt, precipitation, and runoff are abundant (Frei and Schär, 1998; Brunner et al., 2019b; Vorkauf et al., 2021), and released in winter (positive values), when electricity demand is high because of cold temperatures and elevated heating needs (Thornton et al., 2016; Wenz et al., 2017). This regulation seasonality is particularly pronounced in the catchments in the central Alps, which are identified as a first cluster of catchments sharing similar reservoir operation patterns (Figs. 8a and 9a). In this region, reservoirs are mostly operated for hydropower production (Fig. 10; Brunner et al., 2019a). In contrast, reservoir operation seasonality is weaker in the catchments in the pre-Alps and lowland areas (Figs. 8b and 9c), where the second cluster of catchments with similar reservoir operation signals is found. In this region, reservoirs are operated for a wider variety of purposes including flood protection, recreation, energy production, and water and industrial supply (Fig. 10; Speckhann et al., 2021). The catchments belonging to the two clusters clearly differ by elevation and, to a smaller degree, in the catchment area (Fig. 9). That is, high-elevation catchments with melt-dominated streamflow regimes show much stronger regulation signals than low-elevation catchments with rainfall-dominated streamflow regimes (Fig. 8c and d).

4 Discussion

We proposed a generalized additive modelling approach to reconstruct the seasonality and magnitude of reservoir operation using observed streamflow time series, including a period before and after reservoir construction. This statistical approach has the advantage of being observation-based and

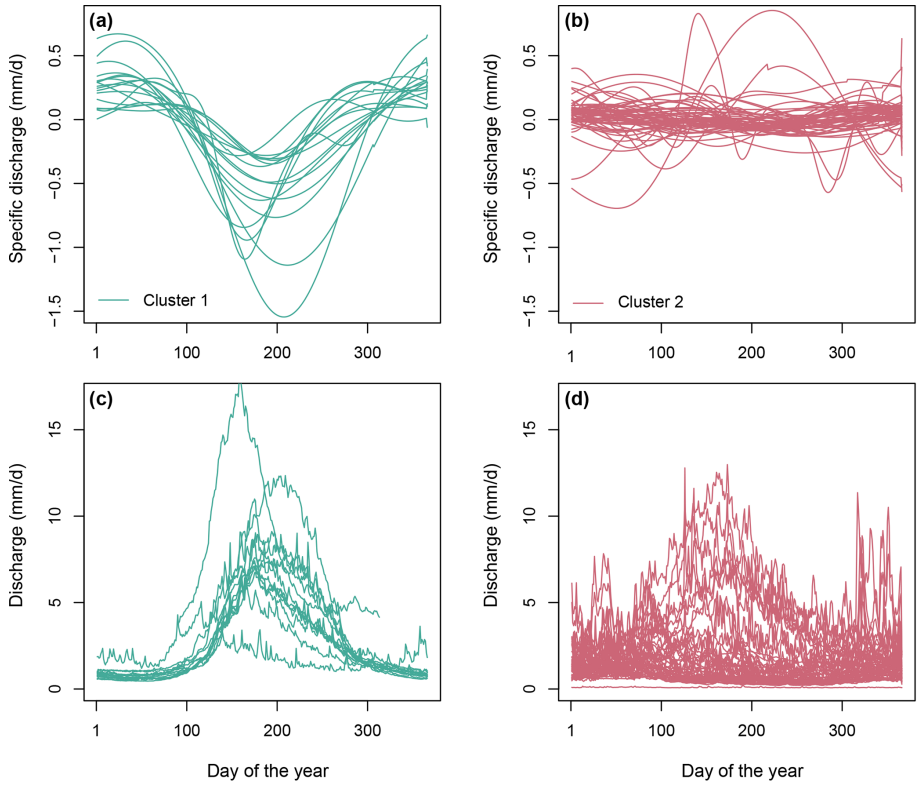

Figure 8. Reservoir regulation seasonality patterns clustered into two groups, namely **(a)** release in winter and storage in summer and **(b)** weak seasonal storage pattern. Natural streamflow regimes (computed using the undisturbed streamflow time series before reservoir construction) belonging to the two reservoir regulation clusters **(c, d)**.

computationally inexpensive. It does not require setting up a hydrological model to simulate natural streamflow. However, the approach also has some limitations. First, it is only applicable in catchments where streamflow observations are available for a natural period before and a regulated period after reservoir construction. This means that the approach is not applicable in ungauged catchments and in catchments where streamflow is only available for a post-reservoir construction period. Turner et al. (2021) proposed a regionalization approach for reservoir operation signals. Our signals may also be regionalized by establishing a relationship between group membership and catchment characteristics, e.g. elevation, which seems to be strongly related to the type of reservoir regulation signal observed (Fig. 8). Second, while the predictive performance of the GAM is satisfactory, there is room for improvement with respect to the simulation of extreme events, which are, as in other approaches, not perfectly represented. The residuals not only represent the reservoir operation signal but also include residual model error. Nonetheless, by smoothing the residuals, we are able to reconstruct a regular pattern representing reservoir regulation. As an alternative to GAMs, we tested the use of generalized additive models for location, scale, and shape (GAMlss) which are said to be more appropriate for modelling time series following extreme value distributions. However, such a model adaptation did not improve the model performance, and new statistical modelling frameworks are needed to better represent extreme events. Third, separating flow changes induced by reservoir operation and other types of changes induced by climate change, such as glacier melt contributions, is challenging. While the GAM representing natural conditions can theoretically consider changes in glacier melt contributions by including glacier mass balance changes, these effects are in practice not perfectly represented because glacier mass balance changes are observed and simulated at a coarse resolution (annual). This means that the signal reconstructed by comparing the simulated natural signal with the observed regulated signal may not solely represent reservoir operation but, to some degree, also changes in glacier melt contributions that are not accounted for by the model. A better separation of the confounding changes – glacier melt and reservoir operation – may be achieved if more detailed information about glacier mass balance were available or in cases where the seasonality of reservoir regulation is clearly different from the seasonality of glacier melt.

The GAM approach proposed here can be used to reconstruct reservoir operation signals in other parts of the world, given that streamflow and climate data are available for a period before and after a known date of reservoir construction. Depending on the hydro-climate, the type of predictors

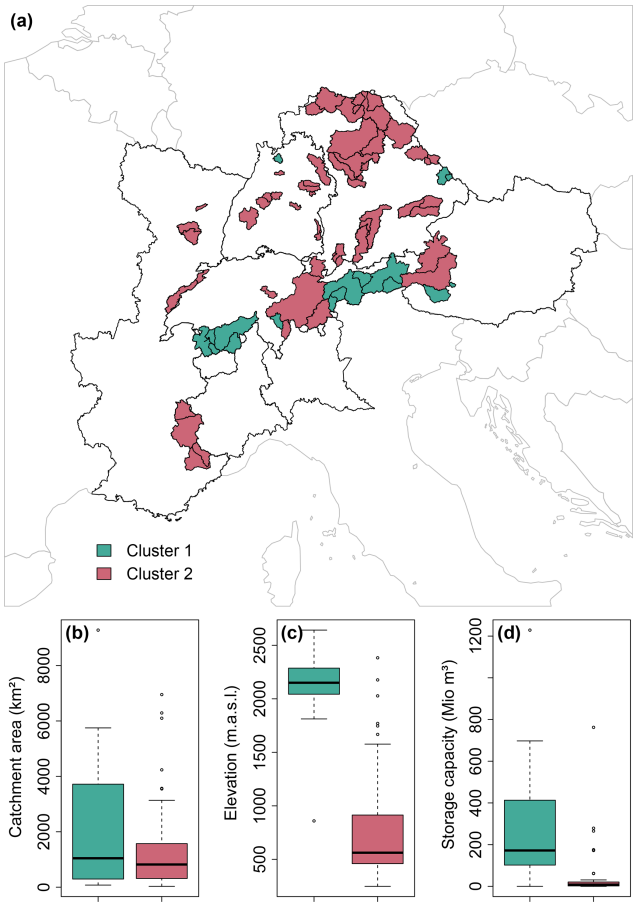

Figure 9. Two groups of catchments with distinct reservoir regulation signals, where panel **(a)** shows catchments belonging to clusters 1 (turquoise) and 2 (red) with similar seasonal regulation patterns (see Fig. 8). Panel **(b)** shows distributions of catchment areas for clusters 1 and 2, **(c)** distributions of elevations for clusters 1 and 2, and **(d)** distributions of reservoir storage capacities for clusters 1 and 2.

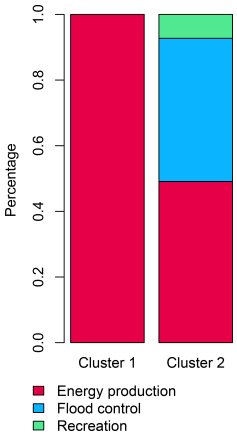

Figure 10. Reservoir purpose mix of catchments in regulation clusters 1 and 2 (see Fig. 9), including energy production, flood control, and recreational use.

used in the GAM might need to be adjusted. For example, the glacier melt part can be removed in non-alpine regions where streamflow is uninfluenced by glacier melt. The GAM modelling approach introduced here can also be used to assess changes in reservoir operation over time. Such an adaptation in reservoir operation might be necessary to account for changing environmental conditions (Feng et al., 2017).

By applying our GAM model to 74 regulated catchments in the central Alps, we are able to show how reservoir regulation seasonality varies in space. We identify two main groups of regulated catchments (Fig. 9), namely those in the central Alps, with storage in summer and release in winter, and those in the pre-Alps and lowland regions, with a less-pronounced operation seasonality and generally weaker storage and release cycles (Fig. 8). The catchments with pronounced regulation cycles in group 1 are mainly operated for hydropower production (Fig. 10), while those with less-pronounced regulation seasonality in group 2 are operated for a variety of purposes such as flood control or recreation (Fig. 10). This finding that lowland catchments have weak reservoir regulation seasonality is in line with findings by Eisele et al. (2004), who have shown that reservoir regulations in Baden-Württemberg, Germany, have a very small impact on the timing of hydrological extremes. Applied at a larger or even global scale, the GAM approach could help us to even better understand spatial variations in reservoir operation.

5 Conclusions

We develop a generalized additive modelling approach using climate variables as predictors to extract reservoir operation signals from observed streamflow time series available for a period before and after reservoir construction. We apply this approach to a set of 74 regulated catchments in the Alps to extract reservoir regulation signals at daily resolution by comparing simulated natural flow with observed regulated flow. The mean reservoir operation seasonalities derived from these daily signals are grouped using functional data clustering to identify groups of catchments with similar reservoir operation strategies. We find that, in the central Alps, there are two groups of catchments with distinct reservoir operation strategies, i.e. high-elevation catchments with pronounced seasonal water redistribution from summer to winter for hydropower production and low-elevation catchments with weak seasonal water redistribution for different reservoir purposes. The reservoir signals reconstructed using the GAM modelling approach may be used to inform hydrological model development and calibration. Furthermore, the reconstructed signals could inform the representation of reservoir operation in hydrological models. Improving this representation is crucial for advancing the field of change attribution, as it will allow for a better separation of climate and

regulation signals, which both influence streamflow characteristics.

Appendix A: Catchments

Table A1. Catchment characteristics of the 74 Alpine catchments used in the analysis, including country, name of river, location of gauging station, record length (years), catchment area (km^2), elevation (m a.s.l.), and start year of reservoir operation.

Country	River	Station	Record length	Start date of record	Catchment area	Elevation reservoir operation	Start year of
CH	Rhône	Porte du Scex	115	1905	5224	2124	1957
CH	Rhône	Sion	104	1916	3363	2287	1957
CH	Rhône	Branson	79	1941	3718	2231	1957
CH	Inn	Martina	116	1904	1936	2342	1968
CH	Muota	Ingenbohl	103	1917	316	1363	1966
CH	Brenno	Loderio	116	1904	399	1812	1963
CH	Dranse de Bagnes	Le Châble, Villette	109	1911	253	2601	1956
CH	Doubs	Ocourt	99	1921	1272	960	1953
CH	Spöl	Punt dal Gall	69	1951	294	2390	1968
CH	Inn	Tarasp	63	1957	1577	2383	1968
CH	Doubs	Combe des Sarrasins	67	1949	996	985	1953
CH	Vispa	Visp	117	1903	784	2642	1965
CH	Moesa	Lumino, Sassello	108	1912	471	1667	1958
AT	Rhein	Lustenau (Höchster Brücke)	66	1951	6289	1770	1976
AT	Bregenzerach	Kennelbach	66	1951	826	1120	1979
AT	Vils	Vils (Lände)	56	1961	198	1274	1965
AT	Inn	Prutz	66	1951	2454	2284	1966
AT	Inn	Magerbach	66	1951	5091	2212	1966
AT	Inn	Innsbruck (above Sill)	66	1951	5750	2139	1981
AT	Ziller	Zell am Ziller – Zellbergeben	66	1951	695	2056	1969
AT	Inn	Kirchbichl – Bichlwang	66	1951	9279	1941	1986
AT	Salzach	Golling	66	1951	3547	1577	1958
AT	Salzach	Oberndorf	56	1961	6099	1340	1974
AT	Mur	Muhr	56	1961	76	2043	1991
AT	Möll	Kolbnitz at the Tauernbahn	46	1971	1045	1935	1981
FR	La Moselle	Remiremont	50	1970	627	724	1983
FR	La Moselle	Épinal	50	1970	1214	653	1983
FR	La Plaine	Raon-l'Étape	50	1970	117	514	1986
FR	La Durance	La Durance à Briançon	62	1955	202	2150	2000
FR	La Durance	La Durance à l' Argentière-la-Bessée	111	1910	961	2177	1966
FR	La Durance	La Durance à Espinasses (Serre-Ponçon)	69	1948	3567	2028	1966
FR	La Tinée	La Tinée à la Tour (Pont de La Lune)	44	1972	703	1746	2006
FR	Le Var	Le Var à Malaussène (La Mescla)	51	1965	1824	1482	2006
DE	Baierzer Rot	Achstetten	96	1924	264	631	1971
DE	Jagst	Schwabsberg	79	1941	178	514	1968
DE	Würm	Schafhausen	68	1952	237	492	1976
DE	Rot	Binnrot	60	1960	130	679	1971
DE	Nagold	Nagold	52	1941	376	625	1965
DE	Kinzig	Schwaibach	106	1914	952	604	1978
DE	Erms	Riederich	98	1922	159	637	1962
DE	Rems	Schorndorf	89	1931	417	432	2006
DE	Zaber	Hausen	89	1931	108	257	1968
DE	Schwarzbach	Eschelbronn	64	1954	191	248	2000
DE	Lauter	Süßen	79	1941	68	562	1976
DE	Lein	Abtsgmünd	99	1921	246	492	1957
DE	Jagst	Dörzbach	97	1923	1027	458	1958

Table A1. Continued.

Country	River	Station	Record length	Start date of record	Catchment area	Elevation reservoir operation	Start year of
DE	Nagold	Calw	79	1941	586	603	1965
DE	Rottach	Greifenmühle	63	1957	31	914	1984
DE	Wertach	Biessenhofen	100	1920	444	884	1959
DE	Altmühl	Treuchtlingen	91	1929	990	469	1974
DE	Altmühl	Eichstätt	91	1929	1391	482	1974
DE	Naab	Unterköblitz	80	1940	2002	514	1965
DE	Schwarzach	Warnbach	80	1940	819	551	1960
DE	Schwarzer Regen	Teisnach Schwarzer Regen	90	1930	624	782	1976
DE	Kleiner Regen	Lohmannmühle	59	1961	116	859	1976
DE	Chamb	Furth im Wald	70	1950	279	540	1989
DE	Chamb	Kothmaißling	60	1960	408	522	1989
DE	Amper	Fürstenfeldbruck	100	1920	1248	744	1961
DE	Amper	Inkofen	95	1925	3135	622	1961
DE	Maisach	Bergkirchen	85	1935	1581	705	1961
DE	Vils	Rottersdorf	81	1939	722	475	1972
DE	Vils	Grafenmühle	81	1939	1433	443	1972
DE	Rott	Birnbach	90	1930	854	460	1960
DE	Main	Schwürbitz	80	1940	2414	488	1968
DE	Main	Kemmern	90	1930	4235	434	1968
DE	Rodach	Unterlangenstadt	90	1930	712	530	1968
DE	Itz	Coburg	95	1925	363	458	1982
DE	Itz	Schenkenau	53	1967	505	423	1982
DE	Regnitz	Pettstadt	98	1922	6951	404	1956
DE	Rednitz	Neumühle Rednitz	110	1910	1816	424	1975
DE	Roth	Roth Bleiche	52	1968	179	414	1985
DE	Pegnitz	Nürnberg Lederersteg	110	1910	1180	457	1956
DE	Fränkische Saale	Bad Kissingen Golfplatz	91	1929	1572	382	1965
DE	Fränkische Saale	Wolfsmünster	90	1930	2116	374	1965

Appendix B: Further model evaluation

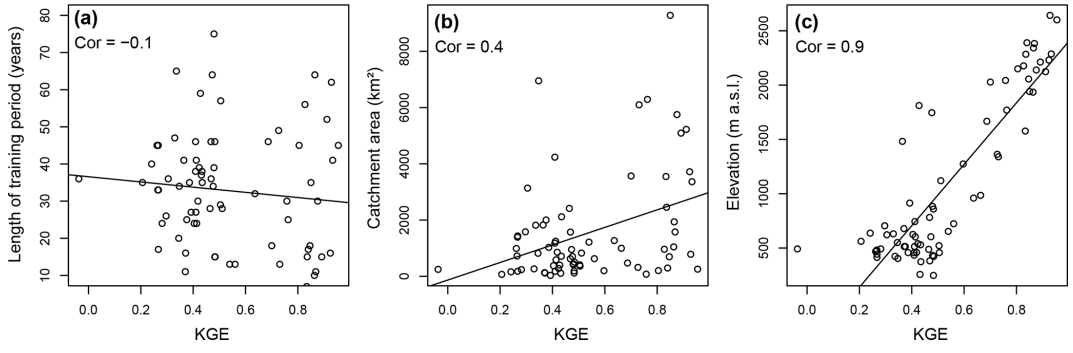

Figure B1. Relationship between model performance and catchment characteristics, including **(a)** record length used to fit the GAM, **(b)** catchment area, and **(c)** elevation.

Data availability. The data used in our analysis are available for download through HydroShare at https://www.hydroshare.org/resource/9007e4a2c68d4df39350af5d1b8b2167/ (Brunner, 2023).

Author contributions. MIB developed the concept and, jointly with PN, the methodology of this study. MIB performed all analyses, produced the figures, and wrote the first draft of the paper, which was revised and edited by PN.

Competing interests. At least one of the (co-)authors is a member of the editorial board of *Hydrology and Earth Systems Sciences*. The peer-review process was guided by an independent editor, and the authors also have no other competing interests to declare.

Disclaimer. Publisher's note: Copernicus Publications remains neutral with regard to jurisdictional claims in published maps and institutional affiliations.

Acknowledgements. We acknowledge the E-OBS dataset, from the EU-FP6 project UERRA (https://www.uerra.eu, last access: 1 March 2022) and the Copernicus Climate Change Service, and the data providers in the European Climate Assessment & Dataset (ECA & D) project; https://www.ecad.eu, last access: 1 March 2022). We thank Loris Compagno, for providing the simulated glacier mass balance time series. In addition, we thank the two anonymous reviewers, for their constructive feedback, which helped to greatly improve the presentation of the results.

Financial support. This research has been supported by the Deutsche Forschungsgemeinschaft (grant no. 2100371301), the French national programmes (FRAISE-LEFE/INSU and 80 PRIME CNRS-INSU), and the European H2020 XAIDA (grant no. 101003469). Philippe Naveau also received support of the French Agence Nationale de la Recherche (ANR; grant no. ANR-20-CE40-0025-01; T-REX project) and the ANR-Melody (grant no. ANR-19-CE46-0011).

This open-access publication was funded
by the University of Freiburg.

Review statement. This paper was edited by Micha Werner and reviewed by Charles Rougé and one anonymous referee.

References

Adam, J. C., Haddeland, I., Su, F., and Lettenmaier, D. P.: Simulation of reservoir influences on annual and seasonal streamflow changes for the Lena, Yenisei, and Ob' rivers, J. Geophys. Res.-Atmos., 112, 1–22, https://doi.org/10.1029/2007JD008525, 2007.

Bard, A., Renard, B., Lang, M., Giuntoli, I., Korck, J., Koboltschnig, G., Janža, M., D'Amico, M., and Volken, D.: Trends in the hydrologic regime of Alpine rivers, J. Hydrol., 529, 1823–1837, https://doi.org/10.1016/j.jhydrol.2015.07.052, 2015.

Biemans, H., Haddeland, I., Kabat, P., Ludwig, F., Hutjes, R. W. A., Heinke, J., Von Bloh, W., and Gerten, D.: Impact of reservoirs on river discharge and irrigation water supply during the 20th century, Water Resour. Res., 47, 1–15, https://doi.org/10.1029/2009WR008929, 2011.

Brunner, M.: Hydro-climatic data for 74 Alpine catchments for a period before and after reservoir construction, HydroShare [data set], https://www.hydroshare.org/resource/9007e4a2c68d4df39350af5d1b8b2167/, last access: 31 January 2023.

Brunner, M. I.: Reservoir regulation affects droughts and floods at local and regional scales, Environ. Res. Lett., 16, 124016, https://doi.org/10.1088/1748-9326/ac36f6, 2021.

Brunner, M. I., Viviroli, D., Furrer, R., Seibert, J., and Favre, A.-C.: Identification of flood reactivity regions via the functional clustering of hydrographs, Water Resour. Res., 54, 2017WR021650, https://doi.org/10.1002/2017WR021650, 2018.

Brunner, M. I., Björnsen Gurung, A., Zappa, M., Zekollari, H., Farinotti, D., and Stähli, M.: Present and future water scarcity in Switzerland: Potential for alleviation through reservoirs and lakes, Sci. Total Environ., 666, 1033–1047, https://doi.org/10.1016/j.scitotenv.2019.02.169, 2019a.

Brunner, M. I., Farinotti, D., Zekollari, H., Huss, M., and Zappa, M.: Future shifts in extreme flow regimes in Alpine regions, Hydrol. Earth Syst. Sci., 23, 4471–4489, https://doi.org/10.5194/hess-23-4471-2019, 2019b.

Brunner, M. I., Newman, A., Melsen, L. A., and Wood, A.: Future streamflow regime changes in the United States: assessment using functional classification, Hydrol. Earth Syst. Sci., 24, 3951–3966, https://doi.org/10.5194/hess-24-3951-2020, 2020.

Brunner, M. I., Slater, L., Tallaksen, L. M., and Clark, M.: Challenges in modeling and predicting floods and droughts: A review, WIREs Water, 8, e1520, https://doi.org/10.1002/wat2.1520, 2021.

Bundesamt für Energie BFE: Elektriziätsstatistik, https://www.bfe.admin.ch/bfe/de/home/versorgung/statistik-und-geodaten/energiestatistiken/elektrizitaetsstatistik.html/ (last access: 1 March 2019), 2022.

Catherine, A., Mouillot, D., Escoffier, N., Bernard, C., and Troussellier, M.: Cost effective prediction of the eutrophication status of lakes and reservoirs, Freshwater Biol., 55, 2425–2435, https://doi.org/10.1111/j.1365-2427.2010.02452.x, 2010.

Chebana, F., Dabo-Niang, S., and Ouarda, T. B. M. J.: Exploratory functional flood frequency analysis and outlier detection, Water Resour. Res., 48, W04514, https://doi.org/10.1029/2011WR011040, 2012.

Coerver, H. M., Rutten, M. M., and Van De Giesen, N. C.: Deduction of reservoir operating rules for application in global

hydrological models, Hydrol. Earth Syst. Sci., 22, 831–851, https://doi.org/10.5194/hess-22-831-2018, 2018.

Coleman, D., Bevitt, R., and Reinfelds, I.: Predicting the thermal regime change of a regulated snowmelt river using a generalised additive model and analogue reference streams, Environ. Process., 8, 511–531, https://doi.org/10.1007/s40710-021-00501-7, 2021.

Compagno, L., Eggs, S., Huss, M., Zekollari, H., and Farinotti, D.: Brief communication: Do 1.0, 1.5, or 2.0 °C matter for the future evolution of Alpine glaciers?, The Cryosphere, 15, 2593–2599, https://doi.org/10.5194/tc-15-2593-2021, 2021.

Cornes, R. C., van der Schrier, G., van den Besselaar, E. J. M., and Jones, P. D.: An ensemble version of the E-OBS temperature and precipitation data sets, J. Geophys. Res.-Atmos., 123, 9391–9409, https://doi.org/10.1029/2017JD028200, 2018.

Criss, R. E. and Winston, W. E.: Do Nash values have value? Discussion and alternate proposals, Hydrol. Process., 22, 2723–2725, https://doi.org/10.1002/hyp.7072, 2008.

Cuevas, A.: A partial overview of the theory of statistics with functional data, J. Stat. Plan. Infer., 147, 1–23, https://doi.org/10.1016/j.jspi.2013.04.002, 2014.

Du, T. L. T., Lee, H., Bui, D. D., Graham, L. P., Darby, S. D., Pechlivanidis, I. G., Leyland, J., Biswas, N. K., Choi, G., Batelaan, O., Bui, T. T. P., Do, S. K., Tran, T. V., Nguyen, H. T., and Hwang, E.: Streamflow prediction in highly regulated, transboundary watersheds using multi-basin modeling and remote sensing imagery, Water Resour. Res., 58, e2021WR031191, https://doi.org/10.1029/2021wr031191, 2022.

Ehsani, N., Fekete, B. M., Vörösmarty, C. J., and Tessler, Z. D.: A neural network based general reservoir operation scheme, Stoch. Environ. Res. Risk Assess., 30, 1151–1166, https://doi.org/10.1007/s00477-015-1147-9, 2016.

Eisele, M., Steinbrich, A., and Leibundgut, C.: Assessment of the human impact on the temporal variability of stream flow in mesoscale river basins, in: Hydrology: Science & Practice for the 21st Century, Vol. II, British Hydrological Society, 375–382, 2004.

Eldardiry, H. and Hossain, F.: Understanding reservoir operating rules in the transboundary Nile river basin using macroscale hydrologic modeling with satellite measurements, J. Hydrometeorol., 20, 2253–2269, https://doi.org/10.1175/JHM-D-19-0058.1, 2019.

Febrero-Bande, M. and Oviedo de la Fuente, M.: Statistical computing in functional data analysis: The R package fda.usc, J. Stat. Softw., 51, 1–3, https://doi.org/10.18637/jss.v051.i04, 2012.

Feng, M., Liu, P., Guo, S., Shi, L., Deng, C., and Ming, B.: Deriving adaptive operating rules of hydropower reservoirs using time-varying parameters generated by the EnKF, Water Resour. Res., 53, 6885–6907, https://doi.org/10.1002/2016WR020180, 2017.

Ferrazzi, M., Vivian, R., and Botter, G.: Sensitivity of regulated streamflow regimes to interannual climate variability, Earth's Future, 7, 1206–1219, https://doi.org/10.1029/2019EF001250, 2019.

Frei, C. and Schär, C.: A precipitation climatology of the Alps from high-resolution rain-gauge observations, Int. J. Climatol., 18, 873–900, https://doi.org/10.1002/(SICI)1097-0088(19980630)18:8<873::AID-JOC255>3.0.CO;2-9, 1998.

Gupta, H. V., Kling, H., Yilmaz, K. K., and Martinez, G. F.: Decomposition of the mean squared error and NSE performance criteria: Implications for improving hydrological modelling, J. Hydrol., 377, 80–91, https://doi.org/10.1016/j.jhydrol.2009.08.003, 2009.

Hanasaki, N., Kanae, S., and Oki, T.: A reservoir operation scheme for global river routing models, J. Hydrol., 327, 22–41, https://doi.org/10.1016/j.jhydrol.2005.11.011, 2006.

Hannah, D. M., Smith, B. P. G., Grunell, A. M., and McGregor, G. R.: An approach to hydrograph classification, Hydrol. Process., 14, 317–338, 2000.

Hastie, T. and Tibshirani, R.: Generalized additive models, Stat. Sci., 1, 297–318, 1986.

He, X., Wada, Y., Wanders, N., and Sheffield, J.: Intensification of hydrological drought in California by human water management, Geophys. Res. Lett., 44, 1777–1785, https://doi.org/10.1002/2016GL071665, 2017.

Höllig, K. and Hörner, J.: Approximation and modeling with B-splines, Society for industrial and applied mathematics, Philadelphia, https://doi.org/10.1137/1.9781611972955, 2013.

Hou, J., van Dijk, A., Beck, H., Renzullo, L., and Wada, Y.: Remotely sensed reservoir water storage dynamics (1984–2015) and the influence of climate variability and management at global scale, Hydrol. Earth Syst. Sci., 26, 3785–3803, https://doi.org/10.5194/hess-26-3785-2022, 2022.

Jacques, J. and Preda, C.: Model-based clustering for multivariate functional data, Comput. Stat. Data Anal., 71, 92–106, https://doi.org/10.1016/j.csda.2012.12.004, 2014.

Jamaludin, S.: Streamflow profile classification using functional data analysis: A case study on the Kelantan river basin, in: vol. 1842, The 3rd ISM international statistical conference, Kuala Lumpur, Malaysia, 1–11, https://doi.org/10.1063/1.4982836, 2016.

Laaha, G., Gauster, T., Tallaksen, L. M., Vidal, J.-P., Stahl, K., Prudhomme, C., Heudorfer, B., Vlnas, R., Ionita, M., Lanen, H. A. J., Adler, M.-J., Caillouet, L., Delus, C., Fendekova, M., Gailliez, S., Hannaford, J., Kingston, D., Loon, A. F. V., Mediero, L., Osuch, M., Romanowicz, R., Sauquet, E., Stagge, J. H., and Wong, W. K.: The European 2015 drought from a hydrological perspective, Hydrol. Earth Syst. Sci., 21, 3001–3024, https://doi.org/10.5194/hess-21-3001-2017, 2017.

Lehner, B., Czisch, G., and Vassolo, S.: The impact of global change on the hydropower potential of Europe: A model-based analysis, Energy Policy, 33, 839–855, https://doi.org/10.1016/j.enpol.2003.10.018, 2005.

Lehner, B., Liermann, C. R., Revenga, C., Vörömsmarty, C., Fekete, B., Crouzet, P., Döll, P., Endejan, M., Frenken, K., Magome, J., Nilsson, C., Robertson, J. C., Rödel, R., Sindorf, N., and Wisser, D.: High-resolution mapping of the world's reservoirs and dams for sustainable river-flow management, Front. Ecol. Environ., 9, 494–502, https://doi.org/10.1890/100125, 2011.

Mahe, G., Lienou, G., Descroix, L., Bamba, F., Paturel, J. E., Laraque, A., Meddi, M., Habaieb, H., Adeaga, O., Dieulin, C., Chahnez Kotti, F., and Khomsi, K.: The rivers of Africa: Witness of climate change and human impact on the environment, Hydrol. Process., 27, 2105–2114, https://doi.org/10.1002/hyp.9813, 2013.

Merleau, J., Perreault, L., Angers, J.-F., and Favre, A.-C.: Bayesian modeling of hydrographs, Water Resour. Res., 43, W10432, https://doi.org/10.1029/2006WR005376, 2007.

Nash, J. E. and Sutcliffe, I. V.: River flow forecasting through conceptual models Part I – A discussion of principles, J. Hydrol., 10, 282–290, 1970.

Peng, D., Guo, S., Liu, P., and Liu, T.: Reservoir storage curve estimation based on remote sensing data, J. Hydrol. Eng., 11, 165–172, https://doi.org/10.1061/(ASCE)1084-0699(2006)11:2(165), 2006.

Ramsay, J. O. and Silverman, B. W.: Applied functional data analysis: methods and case studies, Springer, New York, https://doi.org/10.1007/b98886, 2002.

Ramsay, J. O., Wickham, H., Graves, S., and Hooker, G.: Package 'fda': Functional data analysis, https://cran.r-project.org/web/packages/fda/fda.pdf (last access: 1 March 2022), 2014.

RGI Consortium: Randolph Glacier Inventory 6.0 – A dataset of global glacier outlines, Tech. rep., RGI, Colorado, USA, https://doi.org/10.7265/N5-RGI-60, 2017.

Rottler, E., Francke, T., Bürger, G., and Bronstert, A.: Long-term changes in central European river discharge for 1869–2016: impact of changing snow covers, reservoir constructions and an intensified hydrological cycle, Hydrol. Earth Syst. Sci., 24, 1721–1740, https://doi.org/10.5194/hess-24-1721-2020, 2020.

Shiau, J. T. and Huang, C. Y.: Detecting multi-purpose reservoir operation induced time-frequency alteration using wavelet transform, Water Resour. Manage., 28, 3577–3590, https://doi.org/10.1007/s11269-014-0688-x, 2014.

Speckhann, G. A., Kreibich, H., and Merz, B.: Inventory of dams in Germany, Earth Syst. Sci. Data, 13, 731–740, https://doi.org/10.5194/essd-13-731-2021, 2021.

Steyaert, J. C., Condon, L. E., Turner, S., and Voisin, N.: ResOpsUS, a dataset of historical reservoir operations in the contiguous United States, Scient. Data, 9, 34, https://doi.org/10.1038/s41597-022-01134-7, 2022.

Ternynck, C., Ali, M., Alaya, B., Chebana, F., Dabo-Niang, S., and Ouarda, T. B. M. J.: Streamflow hydrograph classification using functional data analysis, Am. Meteorol. Soc., 17, 327–344, https://doi.org/10.1175/JHM-D-14-0200.1, 2016.

Thornton, H. E., Hoskins, B. J., and Scaife, A. A.: The role of temperature in the variability and extremes of electricity and gas demand in Great Britain, Environ. Res. Lett., 11, 126843, https://doi.org/10.1088/1748-9326/11/11/114015, 2016.

Tijdeman, E., Hannaford, J., and Stahl, K.: Human influences on streamflow drought characteristics in England and Wales, Hydrol. Earth Syst. Sci., 22, 1051–1064, https://doi.org/10.5194/hess-22-1051-2018, 2018.

Turner, S. W., Steyaert, J. C., Condon, L., and Voisin, N.: Water storage and release policies for all large reservoirs of conterminous United States, J. Hydrol., 603, 126843, https://doi.org/10.1016/j.jhydrol.2021.126843, 2021.

van Oel, P. R., Martins, E. S. P. R., Costa, A. C., Wanders, N., and van Lanen, H. A. J.: Diagnosing drought using the downstreamness concept: the effect of reservoir networks on drought evolution, Hydrolog. Sci. J., 63, 979–990, https://doi.org/10.1080/02626667.2018.1470632, 2018.

Verbunt, M., Groot Zwaaftink, M., and Gurtz, J.: The hydrologic impact of land cover changes and hydropower stations in the Alpine Rhine basin, Ecol. Model., 187, 71–84, https://doi.org/10.1016/j.ecolmodel.2005.01.027, 2005.

Vicente-Serrano, S. M., Zabalza-Martínez, J., Borràs, G., López-Moreno, J. I., Pla, E., Pascual, D., Savé, R., Biel, C., Funes, I., Azorin-Molina, C., Sanchez-Lorenzo, A., Martín-Hernández, N., Peña-Gallardo, M., Alonso-González, E., Tomas-Burguera, M., and El Kenawy, A.: Extreme hydrological events and the influence of reservoirs in a highly regulated river basin of northeastern Spain, J. Hydrol.: Reg. Stud., 12, 13–32, https://doi.org/10.1016/j.ejrh.2017.01.004, 2017.

Voisin, N., Li, H., Ward, D., Huang, M., Wigmosta, M., and Leung, L. R.: On an improved sub-regional water resources management representation for integration into earth system models, Hydrol. Earth Syst. Sci., 17, 3605–3622, https://doi.org/10.5194/hess-17-3605-2013, 2013.

Volpi, E., Di Lazzaro, M., Bertola, M., Viglione, A., and Fiori, A.: Reservoir effects on flood peak discharge at the catchment scale, Water Resour. Res., 54, 9623–9636, https://doi.org/10.1029/2018WR023866, 2018.

Vorkauf, M., Marty, C., Kahmen, A., and Hiltbrunner, E.: Past and future snowmelt trends in the Swiss Alps: the role of temperature and snowpack, Climatic Change, 165, 44, https://doi.org/10.1007/s10584-021-03027-x, 2021.

Wan, W., Zhao, J., Li, H., Mishra, A., Leung, L. R., Hejazi, M., Wang, W., Lu, H., Deng, Z., Demissisie, Y., and Wang, H.: Hydrological drought in the Anthropocene: Impacts of local water extraction and reservoir regulation in the U.S., J. Geophys. Res.-Atmos., 122, 11313–11328, https://doi.org/10.1002/2017JD026899, 2017.

Wang, W., Li, H. Y., Leung, L. R., Yigzaw, W., Zhao, J., Lu, H., Deng, Z., Demisie, Y., and Blöschl, G.: Nonlinear filtering effects of reservoirs on flood frequency curves at the regional scale, Water Resour. Res., 53, 8277–8292, https://doi.org/10.1002/2017WR020871, 2017.

Ward, J. H.: Hierarchical grouping to optimize an objective function, J. Am. Stat. Assoc., 58, 236–244, https://doi.org/10.1080/01621459.1963.10500845, 1963.

Wenz, L., Levermann, A., and Auffhammer, M.: North–south polarization of European electricity consumption under future warming, P. Natl. Acad. Sci. USA, 114, E7910–E7918, https://doi.org/10.1073/pnas.1704339114, 2017.

White, M. A., Schmidt, J. C., and Topping, D. J.: Application of wavelet analysis for monitoring the hydrologic effects of dam operation: Glen canyon dam and the Colorado River at lees ferry, Arizona, River Re. Appl., 21, 551–565, https://doi.org/10.1002/rra.827, 2005.

Wood, S.: mgcv: Mixed GAM Computation Vehicle with Automatic Smoothness Estimation, https://stat.ethz.ch/R-manual/R-devel/library/mgcv/html/mgcv-package.html, last access: 1 March 2022.

Wood, S. N.: Generalized additive models. An introduction with R, in: 2nd Edn., CRC Press, Boca Raton, https://doi.org/0.1201/9781315370279, 2017.

Yassin, F., Razavi, S., Elshamy, M., Davison, B., Sapriza-Azuri, G., and Wheater, H.: Representation and improved parameterization of reservoir operation in hydrological and land-surface models, Hydrol. Earth Syst. Sci., 23, 3735–3764, https://doi.org/10.5194/hess-23-3735-2019, 2019.